Magnetic phase diagram for a nonextensive system: Experimental connection with manganites

M. S. Reis* and V. S. Amaral
Departamento de Física and CICECO, Universidade de Aveiro, 3810-193 Aveiro, Portugal

J. P. Araújo
IFIMUP, Departamento de Física, Universidade do Porto, 4150 Porto, Portugal

I. S. Oliveira
Centro Brasileiro de Pesquisas Físicas, Rua Dr. Xavier Sigaud 150 Urca, 22290-180 Rio de Janeiro-RJ, Brazil
(Received 14 January 2003; revised manuscript received 7 April 2003; published 7 July 2003)

In the present paper we make a thorough analysis of a classical spin system, within the framework of Tsallis nonextensive statistics. From the analysis of the generalized Gibbs free energy, within the mean-field approximation, a paramagnetic-ferromagnetic phase diagram, which exhibits first- and second-order phase transitions, is built. The features of the generalized and classical magnetic moment are mainly determined by the values of q, the nonextensive parameter. The model is successfully applied to the case of $La_{0.60}Y_{0.07}Ca_{0.33}MnO_3$ manganite. The temperature and magnetic field dependence of the experimental magnetization on this manganite are faithfully reproduced. The agreement between rather ''exotic'' magnetic properties of manganites and the predictions of the q statistics comes to support our initial claim that these materials are magnetically nonextensive objects.

DOI: 10.1103/PhysRevB.68.014404 PACS number(s): 75.10.Hk, 75.47.Lx, 05.70.Fh

I. INTRODUCTION

In the literature of manganites, various models have appeared as different attempts to reproduce the electric and magnetic properties of these systems. Krivoruchko *et al.*,[1] Núñez-Regueiro and Kadin,[2] and Dionne[3] gave interesting examples of multiparameter models, but failed to achieve full agreement with experimental data. Ravindranath *et al.*[4] compared resistivity data in $La_{0.6}Y_{0.1}Ca_{0.3}MnO_3$ to different two-parameter models, which do not agree with each other in the low-temperature range. Other interesting attempts can be found in the work of Rivas *et al.*,[5] Hueso *et al.*,[6] Heremans *et al.*,[7] Pal *et al.*,[8] Philip and Kutty,[9] Szewczyk *et al.*,[10] Viret *et al.*,[11] and Tkachuk *et al.*[12] None of these obtained plain agreement between experiment and theory, irrespective of their number of adjusting parameters and approach.

On the other hand, Tsallis generalized statistics[13–15] has been successfully applied to an impressive number of subjects.[16] The formalism rests on the definition of generalized entropy:[17]

$$S_q = k\frac{1-\sum_i p_i^q}{q-1}, \tag{1}$$

where q is the *entropic parameter*, p_i are probabilities satisfying $\Sigma_i p_i = 1$, and k is a positive constant. The above formula converges to the usual Maxwell-Boltzmann definition of entropy, and to the usual derived thermodynamic functions, in the limit $q \to 1$.[13–17]

For condensed matter problems, applications of Eq. (1) include Ising ferromagnets,[18–20] molecular field approximation,[21,22] Landau diamagnetism,[23] electron-phonon systems and tight-binding-like Hamiltonians,[24,25] metallic[26] and superconductor[27] systems, etc. The first evidence that the magnetic properties of manganites could be described within the framework of Tsallis statistics was presented by Reis *et al.*,[28] followed by an analysis[29] of the unusual paramagnetic susceptibility of $La_{0.67}Ca_{0.33}MnO_3$, measured by Amaral *et al.*[30]

Maximization of Eq. (1) subjected to the constraint of the normalized q expectation value of the Hamiltonian $\hat{\mathcal{H}}$ (Ref. 13)

$$U_q = \frac{\mathrm{Tr}\{\hat{\mathcal{H}}\hat{\rho}^q\}}{\mathrm{Tr}\{\hat{\rho}^q\}} \tag{2}$$

and the usual normalization of the density matrix $\mathrm{Tr}\{\hat{\rho}\} = 1$ yields the following expression for the density matrix $\hat{\rho}$:

$$\hat{\rho} = \frac{1}{Z_q}[1-(1-q)\tilde{\beta}(\hat{\mathcal{H}}-U_q)]^{1/(1-q)}, \tag{3}$$

where

$$Z_q = \mathrm{Tr}[1-(1-q)\tilde{\beta}(\hat{\mathcal{H}}-U_q)]^{1/(1-q)} \tag{4}$$

is the partition function and $\tilde{\beta} = \beta/\mathrm{Tr}\{\hat{\rho}^q\}$. Here, β is the Lagrange parameter associated with the internal energy. However, Eq. (3) can be written in a more convenient form[13–15,28,29] in terms of β^*, defined as $\beta^* = \tilde{\beta}/[1+(1-q)\tilde{\beta}U_q]$. In particular, to analyze the physical system described here, the quantity $1/(k\beta^*)$ will represent the physical temperature scale, as in Refs. 28 and 29. Discussion about the concept of temperature and Lagrange parameters in Tsallis statistics can be found in the literature.[13,14,28,29,31–36] In the present work, the parameter q is restricted to the interval $0 \leqslant q \leqslant 1$, preserving the entropy concavity.[29,37] Finally, the magnetization of a specimen is, accordingly, given by:[13–15,28,29]

$$\mathcal{M}_q = \frac{\mathrm{Tr}\{\hat{\mu}\hat{\rho}^q\}}{\mathrm{Tr}\{\hat{\rho}^q\}}, \tag{5}$$

where $\hat{\mu}$ is the magnetic moment operator.

In this paper we pursue the idea, based on novel experimental and theoretical results, that manganites are magnetically nonextensive objects. This property appears in systems where long-range interactions and/or fractality exist, and such features have been invoked in recent models of manganites, as well as in the interpretation of experimental results. They appear, for instance, in the work of Dagotto and co-workers,[38] who emphasize the role of competition between different phases in the physical properties of these materials. Various authors have considered the formation of microclusters of competing phases[39–44] with *fractal* shapes, randomly distributed in the material (see Ref. 38 and references therein) and the role of *long-range interactions* in phase segregation.[45,46] Important experimental results in this direction have also been reported by Merithew *et al.*[47] Particularly insightful is the work of Satou and Yamanaka,[48] who derived a *Cantor* spectra for the double-exchange Hamiltonian, the basis of theoretical models of manganites.

A major difficulty with Tsallis formulation concerns the physical meaning of the entropic parameter q. In this direction, Beck and Cohen[49] have recently shown that the value of q gives a direct measure of the internal distribution of temperatures in an *inhomogeneous* system. Although their results are not directly applied to magnetic systems, it has been known for some time that manganites are magnetically inhomogeneous systems (see, for instance, Refs. 38 and 50 and references therein). This fact has been explored very recently by Salamon *et al.*,[51] who applied the idea of *distribution* of the inverse susceptibility (which turns out to be equivalent to a distribution of temperatures) to the analysis of the magnetic susceptibility and the effective paramagnetic moment of $La_{0.7}Ca_{0.3}MnO_3$.

In what follows, we present a magnetic model for classical spins (cluster), based on the framework of Tsallis generalized statistics. In the model, we consider that nonextensivity exists in the intracluster interactions, whereas the intercluster interaction remains extensive. This is important to maintain the total magnetization proportional to the number of clusters. Then, the Gibbs free energy is analyzed, within the mean-field approximation, and a series of interesting magnetic features appears as a consequence of nonextensivity. Finally, connection between the model and experimental data obtained from magnetic measurements on some manganite samples is made.

II. CLASSICAL MODEL

Consider a classical spin $\vec{\mu}$ under a homogeneous magnetic field $\vec{H}$. The Hamiltonian $\mathcal{H}$ is given by

$$\mathcal{H} = -\mu H \cos\theta, \tag{6}$$

where θ is the angle between $\vec{\mu}$ and $\vec{H}$. Following the usual Tsallis formalism,[13–15,28,29] the magnetization $\mathcal{M}_q$ can be determined from Eq. (5),

$$\frac{\mathcal{M}_q}{\mu} = \mathcal{L}_q(x) = \frac{1}{(2-q)} \times \begin{cases} 1 - \dfrac{1}{x}, & x > \dfrac{1}{1-q} \\ \coth_q(x) - \dfrac{1}{x}, & x < \dfrac{1}{1-q} \end{cases} \tag{7}$$

where $x = \mu H/kT$, and $\coth_q$ is the generalized q hyperbolic cotangent.[52] The above two-branch function results from the Tsallis cutoff.[14,15,53] It is interesting to note the similarity between the above result and the traditional Langevin function. In what follows, Eq. (7) will be called *generalized Langevin function*, and this result can also be derived from the *generalized Brillouin function*, introduced in Ref. 29, taking the limit of large spin values ($S \to \infty$). The result derived above is valid only for $0 \leqslant q \leqslant 1$.

The generalized paramagnetic susceptibility χ_q exhibits the usual dependence on the inverse of the absolute temperature

$$\chi_q = \lim_{H \to 0}\left[\frac{\partial \mathcal{M}_q}{\partial H}\right] = \frac{q\mu^2}{3kT} = q\chi_1 \tag{8}$$

and is proportional to the usual paramagnetic Langevin susceptibility χ_1. A similar result was deduced for the generalized Brillouin function.[29]

III. MEAN-FIELD APPROXIMATION

A. Gibbs free energy

The Gibbs free energy is, within the mean field approximation,

$$G = \frac{kT}{\mu}\int_0^{\mathcal{M}_q} \mathcal{M}_q^{-1}(\mathcal{M}_q')\, d\mathcal{M}_q' - H\mathcal{M}_q - \frac{\lambda}{2}\mathcal{M}_q^2, \tag{9}$$

where the first term is the entropy, with $\mathcal{M}_q^{-1}$ the inverse of the generalized Langevin function [Eq. (7)], the second is the Zeeman term, and the third, the exchange energy, with λ as the mean-field parameter. The equilibrium magnetization can be found from the minimization of the Gibbs free energy and, depending on the q value, first- or second-order transition features emerge. At zero magnetic field and for $q > 0.5$ the free energy presents, for any value of temperature, only one minimum, for positive values of magnetization. Correspondingly, a second-order paramagnetic-ferromagnetic phase transition occurs at $T_C^{(q)} = qT_C^{(1)}$, as sketched in Fig. 1(a). Here, $T_C^{(1)} = \mu^2\lambda/3k$ is the Curie temperature for the standard Langevin model. From now on, we introduce the dimensionless temperature $t = T/T_C^{(1)}$ and field $h = \mu H/kT_C^{(1)}$ parameters.

For $q \leqslant 0.5$ the nature of the phase transition is more complex, presenting a typical behavior of first-order phase transition.[54] As is illustrated in Fig. 1(b), for sufficiently high temperatures ($t > t_{SH}$), only one minimum at $\mathcal{M}_q = 0$ is observed. With decreasing temperature, at $t = t_{SH}$, a second minimum appears with finite magnetization and further lowering the temperature to $t = t_c$, this minimum becomes degenerate, corresponding to $\mathcal{M}_q = 0$. For $t < t_c$ the free energy global minimum occurs for finite magnetization, determining

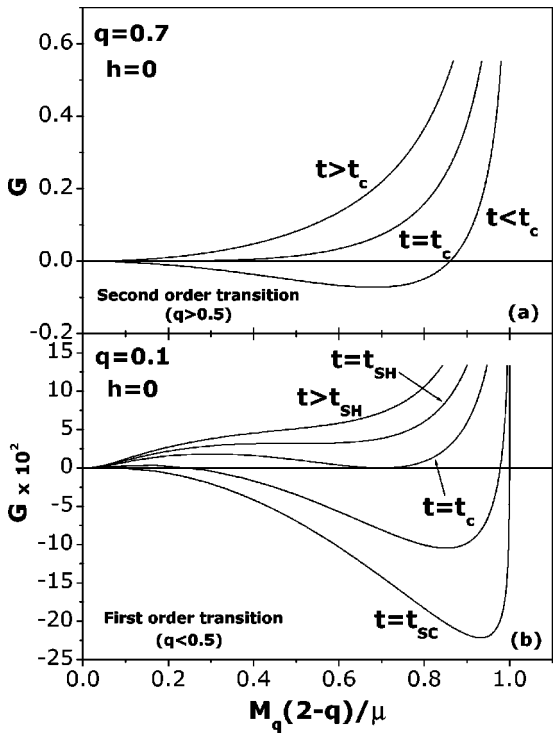

FIG. 1. Gibbs free energy [Eq. (9)], within the mean field approximation and $h=0$, as a function of the reduced magnetization. (a) For $q>0.5$ only one minimum is observed, for any value of temperature ($t>t_c$ or $t<t_c$), representing a second-order phase transition for the magnetization. (b) For $q<0.5$ and $t=t_c$ two degenerate minima are observed, representing a first-order phase transition. The t_{SH} and t_{SC} temperatures limit the superheating-supercooling cycle, responsible for the thermal hysteresis normally observed in first-order phase transitions.

its equilibrium value. However, this equilibrium state is not necessarily the one observed in finite times, since there is an energy barrier between the two minima, which prevents the whole system to reach the global minimum of energy. The minimum temperature that can sustain zero magnetization is the one corresponding to $t=t_{SC}$, where the energy barrier goes to zero and only one minimum exists at finite magnetization. In a similar way, t_{SH} corresponds to the maximum temperature that can sustain a finite magnetization. This phenomena is the well-known superheating-supercooling cycle and is responsible for the thermal hysteresis normally observed in first-order phase transitions.[54] The t_{SH} and t_{SC} temperatures can be analytically derived from the conditions described above, and are valid only for $q\leqslant 0.5$, yielding

$$t_{SH}=\frac{3}{4}\frac{1}{(2-q)}, \tag{10}$$

$$t_{SC}=q. \tag{11}$$

In contrast, a closed expression for t_c cannot be derived, since it involves transcendental equations. The temperature dependence of the reduced equilibrium magnetization $\mathcal{M}_q(2-q)/\mu$ is sensitive to the features described above, as can be seen in Fig. 2 and inset therein.

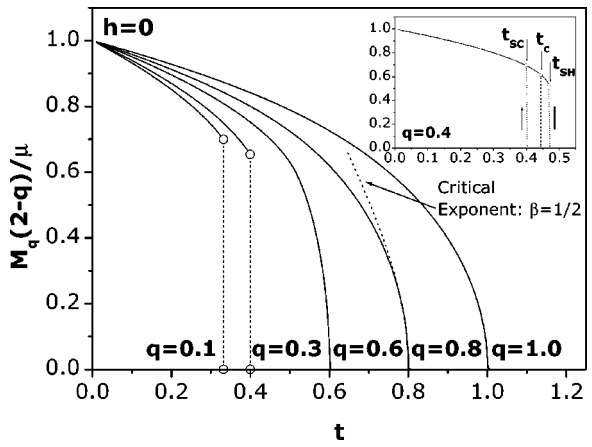

FIG. 2. Temperature dependence of the reduced equilibrium magnetization for several values of q and $h=0$. For $q<0.5$ the transition shows a first-order character, whereas for $q>0.5$ the transition is of second-order type. The dotted line represents the reduced equilibrium magnetization, just below $t=q$, for $q=0.8$, in which the critical exponent $\beta=1/2$ could be obtained [Eq. (31) in Sec. III E]. Inset: Thermal hysteresis normally observed in first-order phase transitions, with the superheating-supercooling cycle.

B. Magnetic susceptibility

The generalized magnetic susceptibiliy χ_q, for any q value, can be derived from Eq. (9),

$$\chi_q=\frac{C^{(q)}}{t-\theta_p^{(q)}}, \tag{12}$$

where

$$C^{(q)}=\frac{\mu}{kT_C^{(1)}}\left[\left.\frac{\partial\mathcal{M}_q^{-1}}{\partial\mathcal{M}_q}\right|_{\mathcal{M}_q(h\to 0,t)}\right]^{-1}. \tag{13}$$

In the paramagnetic phase, $t>t_C$, $\mathcal{M}_q(h\to 0,t)=0$ and the functions $C^{(q)}$ and $\theta_p^{(q)}=\lambda C^{(q)}$ are constants,

$$C^{(q)}=\frac{q}{\lambda}, \tag{14}$$

$$\theta_p^{(q)}=q, \tag{15}$$

resulting in an expression for the *generalized Curie-Weiss law*:

$$\chi_q=\frac{q/\lambda}{t-q}. \tag{16}$$

The temperature dependence of χ_q, and its inverse, is quite distinct, depending whether $q<0.5$ or $q>0.5$, as displayed in Figs. 3(a) and 3(b), respectively. For $q>0.5$ the susceptibility diverges at t_c, the same temperature where its inverse intercepts the temperature axis at $\theta_p^{(q)}$. For $q<0.5$ the susceptibility is always finite and peaks discontinuously at t_c. Correspondingly, its inverse shows a discontinuity with finite values and the Curie-Weiss linear behavior extrapolates to $\theta_p^{(q)}$, which is lower than t_c.

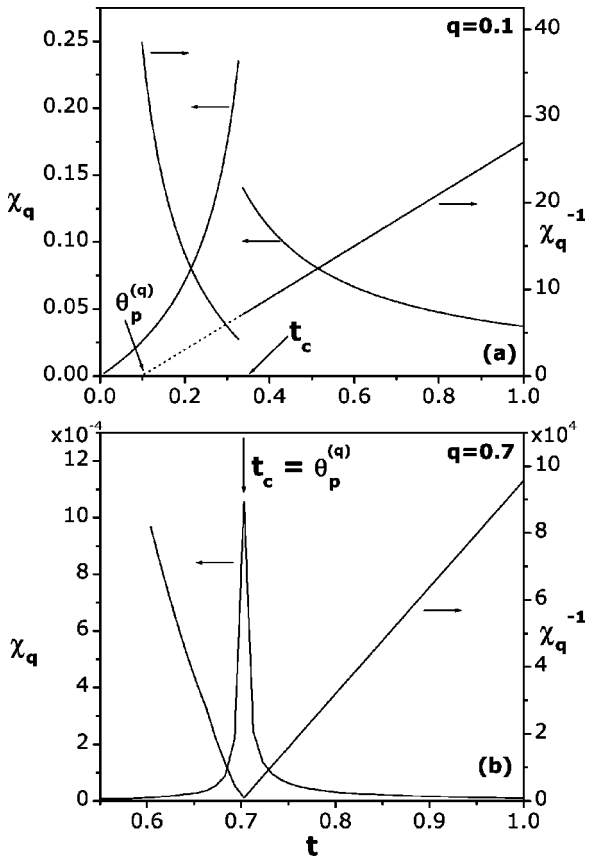

FIG. 3. Temperature dependence of the generalized magnetic susceptibility χ_q, and its inverse, for (a) $q<0.5$ and (b) $q>0.5$.

C. Influence of magnetic field on the magnetization

From the analysis of the Gibbs free energy, we conclude that for $q<0.5$ and $h=0$, the equilibrium magnetization has a first-order phase transition. Sufficiently high magnetic field $h \geqslant h_{0q}$ is able to remove the energy barrier between the two minima in the Gibbs free energy and, consequently, the discontinuity in the equilibrium magnetization curve. This effect is illustrated in Fig. 4. The expression for h_{0q} can be derived from the condition described above, yielding

$$h_{0q}=\frac{3(1-2q)}{2-q}. \tag{17}$$

The quantity $h/\mathcal{M}_q$ is particularly important from the experimental point of view, and is sketched in Fig. 5, for $q<0.5$ and $h=3h_{0q}$. Another interesting point of this model, for $q<0.5$, is the existence of a ferromagnetic phase transition induced by the magnetic field, in the paramagnetic phase. This feature is not related to the growing of the ferromagnetic clusters, since the cluster size is assumed to be constant in the model. In fact, for temperature values sufficiently close to t_c, the two minima of the generalized Gibbs free energy have similar energy values and, consequently, the magnetic field energy plays a decisive role, being able to induce a discontinuous character on the magnetization curve. However, for sufficiently high temperatures $t \geqslant t_{0q}$, only one minimum exists for any value of magnetic field, and the magnetization curve becomes continuous. This effect is illustrated in Fig. 6. The temperature t_{0q}, which determines the continuous or discontinuous nature of the magnetization versus field curve is given by

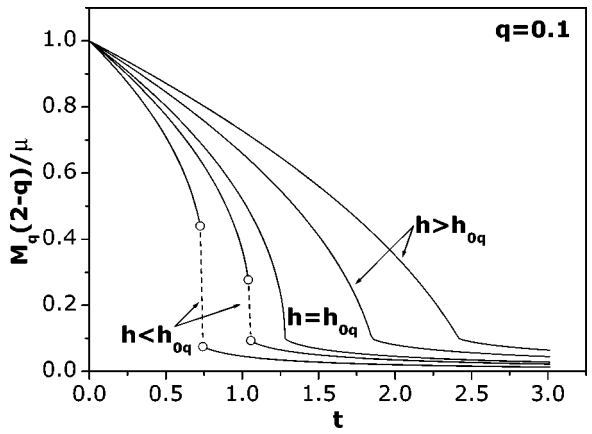

FIG. 4. Temperature dependence of the reduced equilibrium magnetization for several values of h and $q=0.1$. Sufficiently high magnetic field $h \geqslant h_{0q}$ [Eq. (17)], is able to remove the discontinuity in the equilibrium magnetization curve.

$$t_{0q}=\frac{3(1-q)^2}{2-q}. \tag{18}$$

Above t_{0q}, the curves of magnetization as a function of magnetic field are continuous (as described above), presenting, however, a characteristic change of slope at h_c, which in turn varies linearly with temperature:

$$h_c=\alpha(t-t'), \tag{19}$$

where

$$t'=\frac{3q(1-q)}{(2-q)} \tag{20}$$

and

$$\alpha=\frac{1}{1-q}. \tag{21}$$

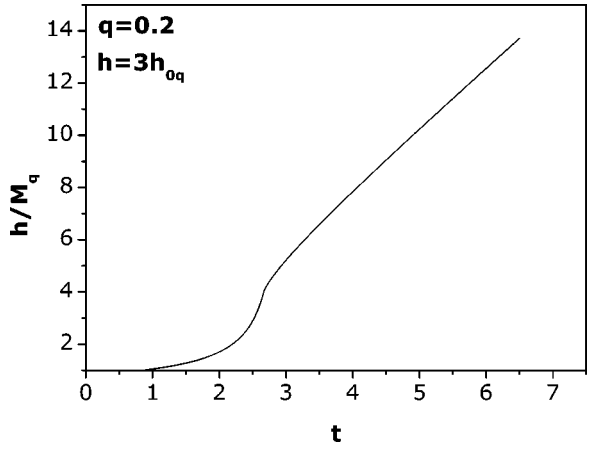

FIG. 5. Temperature dependence of the quantity $h/\mathcal{M}_q$, for $q=0.2$ and $h=3h_{0q}$.

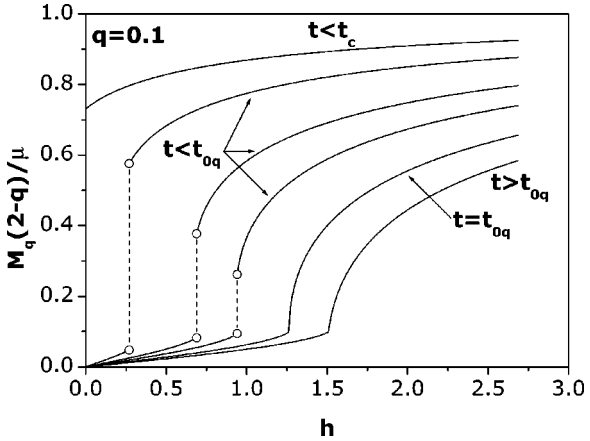

FIG. 6. Magnetic field dependence of the reduced equilibrium magnetization for several values of temperature and $q=0.1$. It represents a ferromagnetic phase transition induced by magnetic field, in the paramagnetic phase. For sufficiently high temperatures $t \geqslant t_{0q}$ [Eq. (18)], the transition becomes continuous.

D. Magnetic phase diagrams

At this point it is convenient to summarize the main properties found so far: the temperature and magnetic field dependence of the generalized magnetization and the generalized magnetic susceptibility depend greatly on the values assumed for the entropic parameter q. It can be the usual second-order paramagnetic-ferromagnetic phase transition but it can become first order, exhibiting the properties normally associated with this type of transition.

Figure 7(a) presents the t-q phase diagram for several values of h. The solid lines divide the plane in ferromagnetic (below) and paramagnetic (above) regions. For $h=0$ and $q>0.5$ the paramagnetic-ferromagnetic phase transition is always second order, whereas for $q<0.5$ the transition becomes first order. The dotted lines limit the irreversibility regions, whereas the shaded areas between the dotted lines represent the ferromagnetic-paramagnetic *phase coexistence*, which can exist for temperatures in the interval $t_{SC}(q) \leqslant t \leqslant t_{SH}(q)$.

Strictly speaking, in the presence of a magnetic field h the ferromagnetic-paramagnetic phase transition does not exist for any temperature, since $\mathcal{M}_q$ is always different from zero. In any case, for $q<0.5$, if the magnetic field is not too high $h<h_{0q}$, the Gibbs free energy presents two minima for temperature values close to t_C and we can always distinguish two phases, one with small magnetization $\mathcal{M}_q^{small}$ and other with large magnetization $\mathcal{M}_q^{large}$. Thus, the phase transition occurs discontinuously, with the shaded areas in Fig. 7(a) corresponding to the values of temperature and q where the phase coexistence occurs. The magnitude of the discontinuity $\Delta\mathcal{M}_q$ decreases with increasing applied magnetic field, disappearing for $h \geqslant h_{0q}$ [Eq. (17)], above which the transition is always continuous (see Fig. 4). However, in this case, the transition occurs with a characteristic slope change in magnetization versus temperature curves, which does not occur for $q>0.5$. The dashed line cuts the transition lines at the point (q_{0h}, t_{0h}), which divides the diagram in two regions:

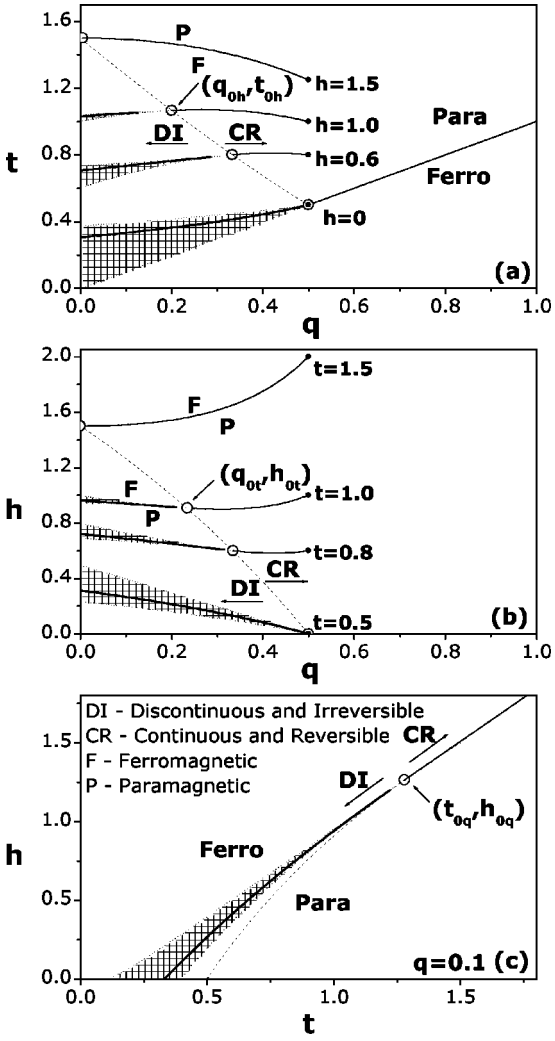

FIG. 7. q magnetic phase diagram summarizing the main properties found in the model. (a) Projection of the phase diagram in the t-q plane. The solid lines divide the plane in ferromagnetic (below) and paramagnetic (above) phases, with a region of phase coexistence between the dotted lines (shaded area). On the left side of the dashed line, the transitions are discontinuous and irreversible (DI), whereas for the right side, the transitions are continuous and reversible (CR) (b) Projection of the phase diagram in the h-q plane, for several temperatures $t>t_c$. The curves in this case are completely analogous to the previous one; however, it is ferromagnetic above the transition lines, since it represents a ferromagnetic transition induced by magnetic field. (c) Projection of the phase diagram in the h-t plane, for $q=0.1$. Above certain values of field $h \geqslant h_{0q}$ [Eq. (17)], and temperature $t \geqslant t_{0q}$ [Eq. (18)], the transition becomes continuous.

one with discontinuous and irreversible (DI) transitions (at left), and other with continuous and reversible (CR) transitions (at right).

As the magnetic field increases, this points travels in the dashed curve according to the parametric equations

$$q_{0h} = \frac{3-2h}{6-h}, \tag{22}$$

$$t_{0h}=\frac{1}{3}\frac{(3+h)^2}{6-h}. \tag{23}$$

In an analogous way, Fig. 7(b) presents the projection of the phase diagram in the h-q plane, for several values of temperature $t>t_c$. Each solid line divides the plane in the ferromagnetic region (above the curve) and in the paramagnetic region (below the curve). For $q<0.5$ and temperature values sufficiently close to t_c, a field-induced phase transition occurs discontinuously, with the shaded areas corresponding to the regions of phase coexistence and irreversibility. The magnitude of the discontinuity $\Delta\mathcal{M}_q$ decreases with increasing temperature, disappearing for $t\geqslant t_{0q}$ [Eq. (18)], above which the transition is always continuous (see Fig. 6). The dashed line cuts the transition curves at the point (q_{0t},h_{0t}), which similarly as in the previous diagram divides it in two regions: one with DI transitions (at left), and other with CR transitions (at right). As the temperature increases, the point moves up along the dashed curve according to the parametric equations given below:

$$q_{0t}=\frac{6-t-\sqrt{t^2+12t}}{6}, \tag{24}$$

$$h_{0t}=\frac{6(t-3+\sqrt{t^2+12t})}{t+6+\sqrt{t^2+12t}}. \tag{25}$$

The projection of the phase diagram in the h-t plane is presented in Fig. 7(c), only for $q=0.1$, for sake of clarity. Again, the dotted lines limit the irreversibility region, and the shaded area represents the values of field and temperature where the two phases can coexist. Above certain values of field $h\geqslant h_{0q}$ and temperature $t\geqslant t_{0q}$, the transition becomes continuous and the characteristic field h_c varies linearly with temperature, as given by Eq. (19). The open circle (t_{0q},h_{0q}) travels along the dashed curve according to Eqs. (17) and (18), and divides the diagram in two regions: one with DI transitions (at left), and other with CR transitions (at right).

E. Generalized Landau coefficients

In this section we derive the generalized coefficients of Landau theory of phase transitions.[54] Let us assume a reduced Gibbs free energy $\mathcal{G}=G/kT_C^{(1)}$ and a reduced magnetization $m=\mathcal{M}_q/\mu$. Thus, we are able to expand, for small values of magnetization, the Gibbs free energy [Eq. (9)], obtaining

$$\mathcal{G}=\frac{\mathcal{A}_q}{2}m^2+\frac{\mathcal{B}_q}{4}m^4+\frac{\mathcal{C}_q}{6}m^6-hm, \tag{26}$$

where

$$\mathcal{A}_q=\frac{3}{q}(t-q), \tag{27}$$

$$\mathcal{B}_q=\frac{9(-3+8q-4q^2)t}{5q^3}, \tag{28}$$

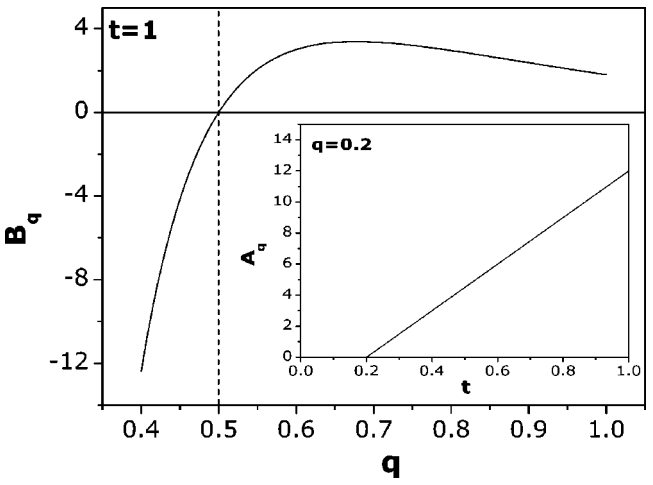

FIG. 8. The generalized Landau coefficient $\mathcal{B}_q$ as a function of the entropic parameter q. For $q<0.5$, $\mathcal{B}_q$ assumes negative values, indicating a first-order phase transition. Inset: temperature dependence of the coefficient $\mathcal{A}_q$ that represents the inverse of the generalized susceptibility.

$$\mathcal{C}_q=\frac{27(54-318q+623q^2-464q^3+116q^4)t}{175q^5}. \tag{29}$$

Within Landau theory, negative values of the coefficient $\mathcal{B}$ represent a first-order transition. In this direction, an obvious correlation between the model proposed here and the usual Landau theory is obtained, since for $q<0.5$, the *generalized Landau coefficient* $\mathcal{B}_q$ also assume negative values, as sketched in Fig. 8. Note that for $q<0.5$ our model also predicts a first-order transition. Additionally, still within Landau theory, the coefficient $\mathcal{A}$ usually takes the form $\mathcal{A}=a(T-T_0)$ (Curie law), and this is exactly the relation found for the *generalized Landau coefficient* $\mathcal{A}_q$ [Eq. (27), sketched in the inset of Fig. 8], which represents the inverse of the generalized susceptibility [Eq. (16)].

It is well known[55–57] that, using the classical formulation of the Landau theory (or similar), a negative slope of the isotherm plots h/m vs m^2 (Arrot plot) would indicate a first-order phase transition. Thus, deriving the minimum of the reduced Gibbs free energy $(d\mathcal{G}/dm=0)$, we can express the h/m quantity as

$$\frac{h}{m}=\mathcal{A}_q+\mathcal{B}_q m^2+\mathcal{C}_q(m^2)^2. \tag{30}$$

As expected, for $q<0.5$ the *generalized Arrot plot* has a negative slope, indicating a first-order transition, whereas for $q>0.5$, these plots are straight lines, characteristic of a ferromagnetic second-order phase transition. These features are presented in Figs. 9(b) and 9(c), for $q>0.5$ and $q<0.5$, respectively, whereas Fig. 9(a) represents the $q=1.0$ case.

On the other hand, the critical exponents of the second-order paramagnetic-ferromagnetic phase transition (for $q>0.5$), can be directly derived from the results above. From Eq. (26) and $t\lesssim q$, one can derive

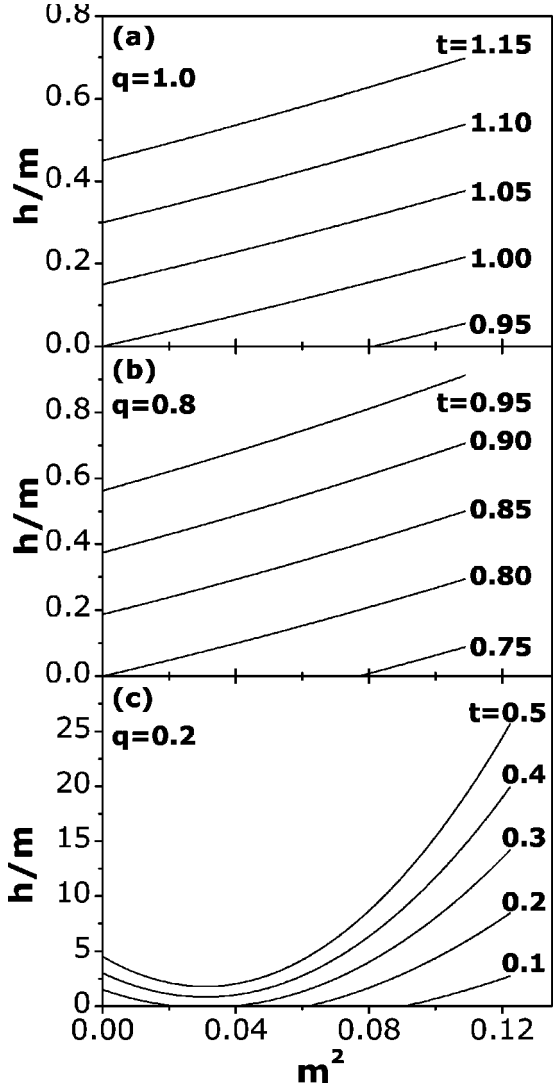

FIG. 9. The generalized Arrot Plot (h/m vs m^2 curves), for (a) $q=1.0$, (b) $q>0.5$, and (c) $q<0.5$.

$$m \simeq F_q \left(\frac{q}{t} - 1 \right)^{1/2}, \tag{31}$$

where

$$F_q = \sqrt{\frac{5}{3} \frac{q^2}{(-3+8q-4q^2)}}. \tag{32}$$

Thus, the critical exponent $\beta=1/2$ describes, at zero field, the temperature dependence of the reduced magnetization m, as represented by the dotted line in Fig. 2, for $q=0.8$. In addition, the critical isotherm, at t_c, of the magnetic field as a function of the reduced magnetization can also be derived from Eq. (26), yielding, for small values of m,

$$h \simeq \frac{3}{F_q^2} m^3 \tag{33}$$

with the critical exponent $\delta=3$. On the other hand, the temperature dependence of the zero-field generalized magnetic susceptibility χ_q can also be obtained from Eq. (26):

$$\chi_q = \{\mathcal{A}_q + 3[m(h \to 0,t)]^2 \mathcal{B}_q\}^{-1}, \tag{34}$$

where $m(h \to 0,t)=0$ for values of temperature slightly above the critical temperature $t \gtrsim t_c$ ($t_c=q$, for $q>0.5$). Thus, the generalized susceptibility becomes

$$\chi_q = \frac{q}{3}(t-q)^{-1}, \tag{35}$$

as described in Eq. (16). On another hand, for $t \lesssim t_c$, $m(h \to 0,t)$ assume the values described in Eq. (31), and the generalized susceptibility becomes

$$\chi_q = \frac{1}{2}\frac{q}{3}(q-t)^{-1}. \tag{36}$$

Note thus that the critical exponent $\gamma=1$, which defines the temperature dependence of the generalized susceptibility around t_c, as well as β and δ, is the same as that describing the mean-field approximation within the Maxwell-Boltzmann statistic.

IV. CONNECTIONS TO EXPERIMENTAL RESULTS

A. A brief survey

The field and temperature dependencies of some manganites present interesting aspects. Mira *et al.*[57,58] analyzed the character of the phase transition in $La_{2/3}(Ca_{1-y}Sr_y)_{1/3}MnO_3$ and concluded that for $y=0$ the magnetic transition is of first order, whereas it is second order for $y=1$. Other works, including those using nuclear magnetic resonance (NMR), support this result.[59,60] Amaral *et al.*[30,61,62] emphasized that $La_{0.67}Ca_{0.33}MnO_3$, $La_{0.8}MnO_3$, and $La_{0.60}Y_{0.07}Ca_{0.33}MnO_3$ exhibit first order transition character, with additional hysteresis for fields below a critical field $H<H_c^*$ and temperature ranges between T_c and a critical temperature T_c^*. For the last manganite cited above, for instance, $M(H)$ presents an upward inflection point from $T_c=150$ K up to 220 K, with a characteristic field $H_c(T)$, for the inflection point, presenting an almost linear temperature dependence. In addition, a large thermal hysteresis is clearly delimited for temperatures ranging from T_c up to the branching point $T_c^* \sim 170$ K. Analogous behavior is found in $La_{0.67}Ca_{0.33}MnO_3$ and $La_{0.8}MnO_3$,[61] $Sm_{0.65}Sr_{0.35}MnO_3$[63], and $Pr_{0.5}Ca_{0.5}Mn_{1-x}Cr_xO_3$ ($x=0.03,\ 0.05$),[64] among others.

Another interesting feature in the magnetization behavior of some manganites concerns the H/M vs T measurement, which presents a strong downturn for values of temperature nearly above T_c. It makes a deviation from the simple Curie-Weiss law, and, at T_c, the magnetic state is quickly switched to a ferromagnetic one. Such a feature is frequently found in the literature of manganites: $La_{0.60}Y_{0.07}Ca_{0.33}MnO_3$ and $La_{0.8}MnO_3$,[62] $Sm_{0.55}Sr_{0.45}MnO_3$,[65,66] $La_{0.825}Sr_{0.175}Mn_{0.86}Cu_{0.14}O_3$,[67] $Ca_{1-x}Pr_xMnO_3$ with $x \leqslant 0.1$,[68] among others.

However, even with the enormous quantity of experimental measurements on manganites (see, for example, the im-

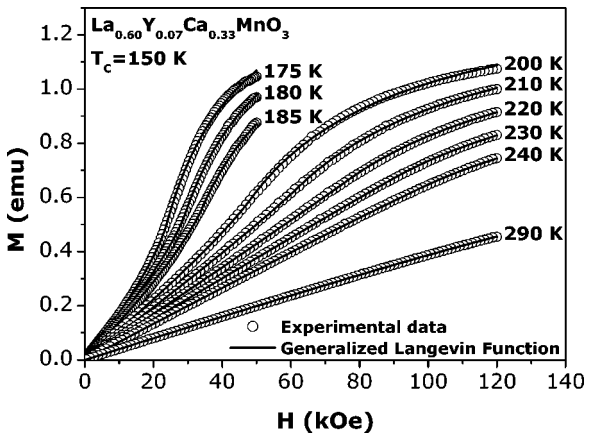

FIG. 10. Measured (open circles) and theoretical [solid lines, Eqs. (7) and (37)] magnetic moment as a function of magnetic field, for several values of temperatures above $T_c = 150$ K.

pressive review written by Dagotto and co-workers[38]), the nature of the phase transition in ferromagnetic manganites is still a controversial issue. In this direction, Amaral *et al.*[61] claim for new models to explain the first-second order character of the transition in manganites, even with the theoretical works developed by Jaime *et al.*,[69] Alonso *et al.*,[70] and Novák *et al.*[59]

To inquire about the order of the phase transition and describe theoretically the behavior of the relevant magnetic quantities, Amaral and co-workers[61,62] used the macroscopic Landau theory of phase transition, expanding the free energy up to sixth power of the magnetization. If the coefficient $\mathcal{B}$ (with respect to M^4) is negative, the transition can be first-order-like. In this case, the magnetization will present a large field cycling irreversibility *only* for values of magnetic field and temperature below H_c^* and T_c^*, respectively. Further analysis of Landau theory, even for $\mathcal{B}<0$ and higher temperatures and magnetic fields ($H>H_c^*$ and $T>T_c^*$), shows that the magnetization has a peculiar inflection point at a characteristic magnetic field H_c that increases linearly with temperature, $H_c(T) \propto (T - T_0)$. However, the results of Landau theory are not sufficient to reproduce all peculiar magnetic properties of the manganites, such as the anomalous behavior of the H/M vs T quantity, presented in Figs. 5 and 12.

B. Experimental and theoretical results for $La_{0.60}Y_{0.07}Ca_{0.33}MnO_3$

Ferromagnetic ceramic $La_{0.60}Y_{0.07}Ca_{0.33}MnO_3$ was prepared by standard solid-state methods[62] and the magnetization was measured using a Quantum Design superconducting quantum interference device (SQUID) magnetometer (55 kOe) and an Oxford Instruments vibrating sample magnetometer (VSM) (120 kOe). In this section we will apply the general results obtained in the previous sections to a quantitative analysis of experimental data for $La_{0.60}Y_{0.07}Ca_{0.33}MnO_3$. As stated in Sec. III, we work within the mean-field approximation, for which x assumes the expression

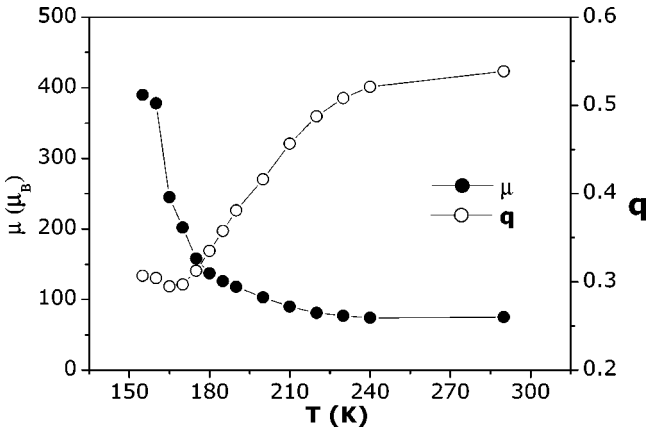

FIG. 11. Temperature dependence of the fitting parameters q and μ (see text).

$$x = \frac{\mu(H + \lambda \mathcal{M}_q)}{kT}, \tag{37}$$

where λ is the mean-field parameter. Figure 10 presents the measured and theoretical magnetic moment as a function of magnetic field, for several values of temperature above T_c. The excellent experimental-theoretical agreement is due to the use of the Tsallis statistics, which parametrizes the system inhomogeneity.[38]

Here, we use q, μ, λ, and N, the number of clusters in the sample, as free parameters. The magnetic moment μ of the clusters follows the usual temperature tendency of a paramagnetic-ferromagnetic transition, whereas q increases towards unity with increasing temperature (Fig. 11). The temperature dependence of the parameter q was expected, since for sufficiently high temperatures there are no clusters, and, consequently, the system becomes extensive ($q = 1.0$).

From these results, we were able to compare the anomalous downturn in H/M vs T curves just with the temperature dependence of q and μ and the approximately constant values of λ and N. The calculated $H/\mathcal{M}_q$ vs T curve is displayed in Fig. 12, with its corresponding experimental value. One

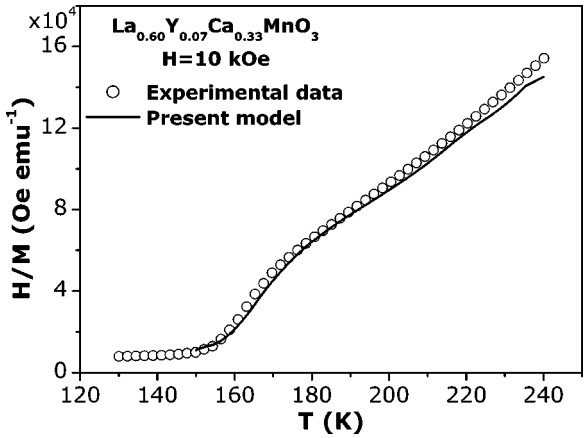

FIG. 12. Measured (open circles) and theoretical (solid line) values of the quantity H/M vs T. The solid line in this plot does not include any fitting parameters, and was calculated using only the fitted parameters obtained from Fig. 10.

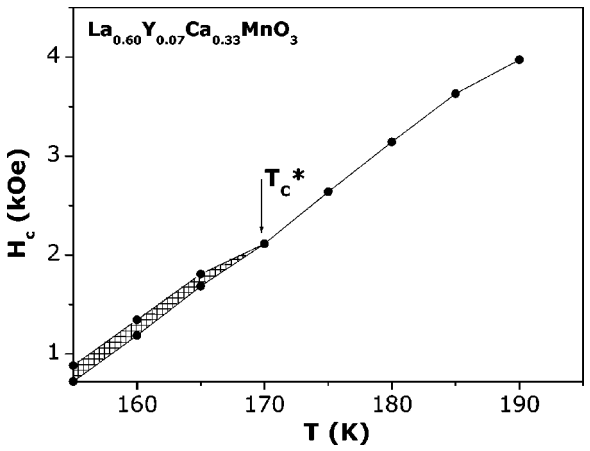

FIG. 13. The linear temperature dependence, for $T>T_c^*$, of the characteristic field H_c, which corresponds to the inflection point of the experimental M vs H curves, measured in $La_{0.60}Y_{0.07}Ca_{0.33}MnO_3$. For $T_c<T<T_c^*$ the hysteresis is indicated by the shaded area. The similarity between this experimental plot and the theoretical one, shown in Fig. 7(c), is striking.

should stress that the solid line in this plot does not include any other fitting parameter. The curve was calculated using only the fitted parameters obtained from Fig. 10.

Additionally, Amaral and co-workers[61] pointed out that the inflection point, at H_c, on the M vs H curves of $La_{0.60}Y_{0.07}Ca_{0.33}MnO_3$ presents two different features: one for $T>T_c^*$, where the characteristic field H_c has a linear temperature dependence, and other for $T_c<T<T_c^*$, where, due the irreversibility, there are two characteristic fields. Figure 13 shows the plot of H_c vs T obtained from experimental data. The similarity is striking between this plot and the curve shown in Fig. 7(c).

Finally, the Arrot plots presented by Amaral *et al.*[61,62] and Mira *et al.*[57,58] are very similar to those presented in Figs. 9(b) and 9(c). In addition, Mohan *et al.*[71] and Lofland *et al.*[72] found for the critical exponents (β,γ,δ), measured in $La_{0.8}Sr_{0.2}MnO_3$, (0.50,1.05,3.13) and (0.5,1.0,−), respectively, as theoretically obtained in Sec. III E. These results contrast with those reported in the literature for $La_{0.8}Sr_{0.2}CoO_3$, (0.46,1.39,4.02), which does not have long-range interactions below the Curie point.[73]

V. CONCLUSION

In two previous publications[28,29] we presented evidence that the magnetic properties of manganites can be suitably described in the framework of Tsallis statistics. In the present paper we have extended our analysis and presented compelling evidence in this direction by deducing a magnetic phase diagram that matches observed experimental results on $La_{0.60}Y_{0.07}Ca_{0.33}MnO_3$, along with some other magnetic properties of this compound. The interpretation of the entropic parameter q, given by Beck and Cohen[49] in terms of the ratio between the mean and width of the temperature distribution in the system, comes to support our proposal, since manganites have long been recognized as objects whose properties are dominated by intrinsic inhomogeneities.[38,50,65] Such a distribution can be translated as a distribution of the magnetic susceptibility, as pointed out by Salamon *et al.*,[51] from which a temperature dependence of q can be expected. Therefore, we conclude that Tsallis nonextensive statistics is a handy tool to study, classify, and predict magnetic and thermal properties of manganites.

ACKNOWLEDGMENTS

The authors thanks FAPERJ/Brazil, FCT/Portugal (Contract No. POCTI/CTM/35462/99) and ICCTI/CAPES (Portugal-Brazil bilateral cooperation), for financial support. We are also thankful to A.P. Guimarães, E.K. Lenzi, and R.S. Mendes for their helpful suggestions.

*Present address: Centro Brasileiro de Pesquisas Físicas, Rua Dr. Xavier Sigaud 150 Urca, 22290-180 Rio de Janeiro-RJ, Brazil; electronic address: marior@fis.ua.pt

[1] V. N. Krivoruchko, S. I. Khartsev, A. D. Prokhorov, V. I. Kamenev, R. Szymczak, M. Baran, and M. Berkowski, J. Magn. Magn. Mater. **207**, 168 (1999).
[2] J. E. Nunez-Regueiro and A. M. Kadin, Appl. Phys. Lett. **68**, 2747 (1996).
[3] G. F. Dionne, J. Appl. Phys. **79**, 5172 (1996).
[4] V. Ravindranath, M. S. Ramachandra, G. Rangarajan, L. Yafeng, J. Klein, R. Klingeler, S. Uhlenbruck, B. Bchner, and R. Gross, Phys. Rev. B **63**, 184434 (2001).
[5] J. Rivas, L. E. Hueso, A. Fondado, F. Rivadulla, and M. A. López-Quintela, J. Magn. Magn. Mater. **221**, 57 (2000).
[6] L. E. Hueso, F. Rivadulla, R. D. Sánchez, D. Caeiro, C. Jardón, C. Vázquez-Vázquez, J. Rivas, and M. A. López-Quintela, J. Magn. Magn. Mater. **189**, 321 (1998).
[7] J. J. Heremans, M. Carris, S. Watts, X. Yu, K. H. Dahmen, and S. von Molnár, J. Appl. Phys. **81**, 4967 (1997).
[8] S. Pal, A. Banerjee, E. Rozenberg, and B. K. Chaudhuri, J. Appl. Phys. **89**, 4955 (2001).
[9] J. Philip and T. R. N. Kutty, J. Phys.: Condens. Matter **11**, 8537 (1999).
[10] A. Szewczyk, H. Szymczac, A. Wisniewski, K. Piotrowski, R. Kartaszynski, B. Dabrowski, S. Kolesnik, and Z. Bukowski, Appl. Phys. Lett. **77**, 1026 (2000).
[11] M. Viret, L. Ranno, and J. M. D. Coey, Phys. Rev. B **55**, 8067 (1997).
[12] A. Tkachuk, K. Rogacki, D. E. Brown, B. Dabrowski, A. J. Fedro, C. W. Kimball, B. Pyles, X. Xiong, D. Rosenmann, and B. D. Dunlap, Phys. Rev. B **57**, 8509 (1998).
[13] C. Tsallis, R. S. Mendes, and A. R. Plastino, Physica A **261**, 534 (1998).
[14] C. Tsallis, in *Nonextensive Statistical Mechanics and Its Applications*, edited by S. Abe and Y. Okamoto (Springer-Verlag, Heidelberg, 2001).
[15] C. Tsallis, Braz. J. Phys. **29**, 1 (1999), available at www.sbf.if.usp.br.
[16] For a complete and updated list of references, see the web site tsallis.cat.cbpf.br/biblio.htm.
[17] C. Tsallis, J. Stat. Phys. **52**, 479 (1988).
[18] R. F. S. Andrade, Physica A **175**, 285 (1991).

[19] R. F. S. Andrade, Physica A **203**, 486 (1994).
[20] U. Tirnakli, D. Demirhan, and F. Buyukkilic, Acta Phys. Pol. A **91**, 1035 (1997).
[21] F. Buyukkilic, U. Tirnakli, and D. Demirhan, Turk. J. Phys. **21**, 132 (1997).
[22] F. Buyukkilic, D. Demirhan, and U. Tirnakli, Physica A **238**, 285 (1997).
[23] S. F. Ozeren, U. Tirnakli, F. Buyukkilic, and D. Demirhan, Eur. Phys. J. B **2**, 101 (1998).
[24] I. Koponen, Phys. Rev. E **55**, 7759 (1997).
[25] L. Borland and J. G. Menchero, Braz. J. Phys. **29**, 169 (1999), available at www.sbf.if.usp.br.
[26] I. S. Oliveira, Eur. Phys. J. B **14**, 43 (2000).
[27] L. H. C. M. Nunes and E. V. L. Mello, Physica A **296**, 106 (2001).
[28] M. S. Reis, J. C. C. Freitas, M. T. D. Orlando, E. K. Lenzi, and I. S. Oliveira, Europhys. Lett. **58**, 42 (2002).
[29] M. S. Reis, J. P. Araújo, V. S. Amaral, E. K. Lenzi, and I. S. Oliveira, Phys. Rev. B **66**, 134417 (2002).
[30] V. S. Amaral, J. P. Araújo, Y. G. Pogorelov, J. M. B. L. dos Santos, P. B. Tavares, A. A. C. S. Lourengo, J. B. Sousa, and J. M. Vieira, J. Magn. Magn. Mater. **226**, 837 (2001).
[31] A. K. Rajagopal, in *Nonextensive Statistical Mechanics and Its Applications*, edited by S. Abe and Y. Okamoto (Springer-Verlag, Heidelberg, 2001).
[32] S. Abe, S. Martinez, F. Pennini, and A. Plastino, Phys. Lett. A **281**, 126 (2001).
[33] S. Abe, Physica A **300**, 417 (2001).
[34] S. Martínez, F. Nicolás, F. Pennini, and A. Plastino, Physica A **286**, 489 (2000).
[35] S. Martínez, F. Pennini, and A. Plastino, Physica A **295**, 246 (2001).
[36] K. Sasaki and M. Hotta, Chaos, Solitons Fractals **13**, 513 (2002).
[37] A. K. Rajagopal and S. Abe, Phys. Rev. Lett. **83**, 1711 (1999).
[38] E. Dagotto, T. Hotta, and A. Moreo, Phys. Rep. **344**, 1 (2001).
[39] M. Mayr, A. Moreo, J. A. Vergés, J. Arispe, A. Feiguin, and E. Dagotto, Phys. Rev. Lett. **86**, 135 (2001).
[40] A. L. Malvezzi, S. Yunoki, and E. Dagotto, Phys. Rev. B **59**, 7033 (1999).
[41] J. W. Lynn, R. W. Erwin, J. A. Borchers, Q. Huang, A. Santoro, J. L. Peng, and Z. Y. Li, Phys. Rev. Lett. **76**, 4046 (1996).
[42] D. E. Cox, P. G. Radaelli, M. Marezio, and S. W. Cheong, Phys. Rev. B **57**, 3305 (1998).
[43] J. M. deTeresa, M. R. Ibarra, P. A. Algarabel, C. Ritter, C. Marquina, J. Blasco, J. Garcia, A. delMoral, and Z. Arnold, Nature (London) **386**, 256 (1997).
[44] J. B. Goodenough and J. S. Zhou, Nature (London) **386**, 229 (1997).
[45] A. Moreo, S. Yunoki, and E. Dagotto, Science **283**, 2034 (1999).
[46] J. Lorenzana, C. Castellani, and C. D. Castro, Phys. Rev. B **64**, 235127 (2001).
[47] R. D. Merithew, M. B. Weissman, F. M. Hess, P. Spradling, E. R. Nowak, J. O'Donnell, J. N. Eckstein, Y. Tokura, and Y. Tomioka, Phys. Rev. Lett. **84**, 3442 (2000).
[48] A. Satou and M. Yamanaka, Phys. Rev. B **63**, 212403 (2001).
[49] C. Beck and E. G. D. Cohen, cond-mat/0205097 (unpublished).
[50] M. S. Reis, V. S. Amaral, P. B. Tavares, A. M. Gomes, A. Y. Takeuchi, A. P. Guimaraes, I. S. Oliveira, and P. Panissod cond-mat/0211143 (unpublished).
[51] M. B. Salamon, P. Lin, and S. H. Chun, Phys. Rev. Lett. **88**, 197203 (2002).
[52] E. P. Borges, J. Phys. A **31**, 5281 (1998).
[53] A. R. Lima and T. J. P. Penna, Phys. Lett. A **256**, 221 (1999).
[54] D. I. Uzinov, *Introduction to the Theory of Critical Phenomena* (World Scientific, Singapore, 1993).
[55] C. P. Bean and D. S. Rodbell, Phys. Rev. **126**, 104 (1962).
[56] S. K. Banerjee, Phys. Lett. **12**, 16 (1964).
[57] J. Mira, J. Rivas, F. Rivadulla, and M. A. López-Quintela, Physica B **320**, 23 (2002).
[58] J. Mira, J. Rivas, F. Rivadulla, C. Vázquez-Vázquez, and M. A. López-Quintela, Phys. Rev. B **60**, 2998 (1999).
[59] P. Novák, M. Marysko, M. M. Savosta, and A. N. Ulyanov, Phys. Rev. B **60**, 6655 (1999).
[60] Y. Tomioka, A. Asamitsu, and Y. Tokura, Phys. Rev. B **63**, 024421 (2000).
[61] V. S. Amaral, J. P. Araújo, Y. G. Pogorelov, J. B. Sousa, P. B. Tavares, J. M. Vieira, P. A. Algarabel, and M. R. Ibarra, J. Appl. Phys. **93**, 7646 (2003).
[62] V. S. Amaral, J. P. Araújo, Y. G. Pogorelov, P. B. Tavares, J. B. Sousa, and J. M. Vieira, J. Magn. Magn. Mater. **242**, 655 (2002).
[63] R. P. Borges, F. Ott, R. M. Thomas, V. Skumryev, J. M. D. Coey, J. J. Amandas, and L. Ranno, Phys. Rev. B **60**, 12847 (1999).
[64] R. Mahendiran, M. Hervieu, A. Maignan, C. Martin, and B. Raveau, Solid State Commun. **114**, 429 (2000).
[65] Y. Tokura and Y. Tomioka, J. Magn. Magn. Mater. **200**, 1 (1999).
[66] J. M. DeTeresa *et al.*, Phys. Rev. B **65**, 100403 (2002).
[67] L. Zheng, X. Xu, L. Pi, and Y. Zhang, Phys. Rev. B **62**, 1193 (2000).
[68] M. M. Savosta, P. Novák, M. Marysko, Z. Jirák, J. Hejtmánek, J. Englich, J. Kohout, C. Martin, and B. Raveau, Phys. Rev. B **62**, 9532 (2000).
[69] M. Jaime, P. Lin, S. H. Chun, M. B. Salamon, P. Dorsey, and M. Rubinstein, Phys. Rev. B **60**, 1028 (1999).
[70] J. L. Alonso, L. A. Fernandez, F. Guinea, V. Laliena, and V. Martin-Mayor, Phys. Rev. B **63**, 054411 (2001).
[71] C. Mohan, M. Seeger, H. Kronmduller, P. Murugaraj, and J. Maier, J. Magn. Magn. Mater. **183**, 348 (1998).
[72] S. E. Lofland, S. M. Bhagat, K. Ghosh, R. L. Greene, S. G. Karabashev, D. A. Shulyatev, A. A. Arsenov, and Y. Mukovskii, Phys. Rev. B **56**, 13705 (1997).
[73] J. Mira, J. Rivas, M. Vázquez, J. M. García-Beneytez, J. Arcas, R. D. Sánchez, and M. A. Senarís-Rodríguez, Phys. Rev. B **59**, 123 (1999).